XX IMEKO World Congress
Metrology for Green Growth
September 9–14, 2012, Busan, Republic of Korea

TIME-INTERVAL MEASUREMENT SYSTEM OF HIGH RESOLUTION IMPLEMENTED IN FPGA DEVICE

M. Zieliński[1], D. Chaberski[2], M. Gurski[3] and M. Kowalski[4]

[1] *Institute of Physics, Nicolaus Copernicus University, Torun, Poland, marziel@fizyka.umk.pl*
[2] *Institute of Physics, Nicolaus Copernicus University, Torun, Poland, daras@fizyka.umk.pl*
[3] *Institute of Physics, Nicolaus Copernicus University, Torun, Poland, gural@fizyka.umk.pl*
[4] *Institute of Physics, Nicolaus Copernicus University, Torun, Poland, markow@fizyka.umk.pl*

Abstract: This paper describes a new time-interval measurement system of high resolution, which contains sixteen multi-tap delay lines. In practice, during single measuring cycle sixteen time-stamps are registered and collected twice. It means that measured time-interval can be precisely interpolated from collection of time-stamps even after each measuring cycle. This solution leads straight to increase of resolution measurements and to limit total duration time of the measurements. Indirectly, such system architecture leads to decrease of duty cycle of the measurement instrument and limits energy consumption which is particularly important in battery powered systems.

Keywords: Time-interval measurement, measurement systems, FPGA applications, QNM method.

1. INTRODUCTION

During last several years in different scientific journals and conference proceedings many times time-interval measurement methods and systems were described and discussed [1 - 4]. Usually, high resolution TIMS (Time-Interval Measurement System) should be characterized by resolution better than 1 ns. Fortunately, modern FPGA devices allow for designing TIMS of resolution much better than 1 ns [5 - 6]. High resolution TIMS are widely applied. System for life-time of the excited atomic states measurement, system for clock characterization, system for quantum cryptography experiments, system for ultrasonic flow-meters or monitoring system of time-of-flight mass spectrometer can be good examples of the single-stage TIMS implemented in the CMOS FPGA devices applications [7, 8]. Of course, it should be noticed, that systems implemented in FPGA devices need relatively much energy. Limiting of the total time of time-interval measurements and increasing at the same time system resolution lead to the decreasing the duty cycle and limiting total power consumption [4].

The measurement system presented in this paper enables not only for increasing the system resolution but also for significantly decreasing uncertainty of the single time-interval measurement.

2. PRINCIPLE OF TIME-INTERVAL MEASUREMENT

The main task of the measuring system is registration and collection of time-stamps corresponding to incoming pulses, which arrived at the “Start” and “Stop” inputs. The measured time-interval is calculated using collection of the time-stamps. The system can work in simple Start / Stop mode or in multi-Stop mode. Most of high resolution TIMS uses the measurement method shown in Fig.1 [1, 4]. In this method the measured time-interval is divided for three time intervals, which are separately measured:

1. Δt_p - between the stop pulse rise transition and clock rise transition,
2. Δt_k - between the start pulse rise transition and clock rise transition,
3. Δt_N - which consists of the integer number N of standard clock periods ($\Delta t_N = NT_0$).

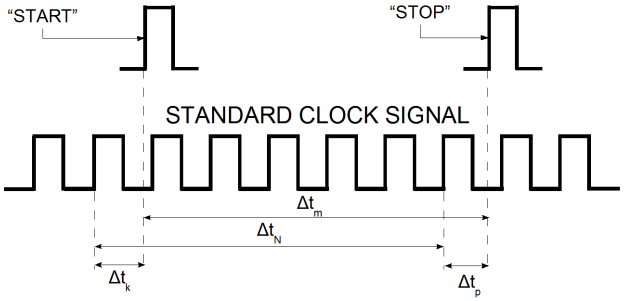

Fig.1. Principle of time-interval measurement

Usually integer number of clock cycles is counted by two counters of which first is incremented by the clock rise transition and the second by the clock fall transition. The result of time-interval measurement will be given as:

$$\Delta t_m = \Delta t_N + \Delta t_p - \Delta t_k = \Delta t_p - \Delta t_k + NT_0 \qquad (1)$$

Precision of TIMS in practice depends on the precision of interpolators, that measure residual time intervals Δt_p, Δt_k and accumulated jitter of standard clock, which is used to determine of time-interval Δt_N. In case of small range of

measured time-intervals (10 ns – 10 μs), for example: measurement of small flow or time-of-flight in mass spectrometry, precision of the measurement depends in practice on measurement of residual time intervals Δt_p, Δt_k [4]. Precision of measurement Δt_p and Δt_k depends on type of interpolator which is applied in the TIMS. If multi-tap delay lines are used in the design of interpolator then value of the single segment delays τ and its standard deviation σ_τ determines precision $\sigma_{\Delta t}$ of time-interval Δt_m measurement. If interpolator consists of n delay lines of relatively high resolution, then during the single measuring cycle it is possible to obtain n different results of Δt_m measurement. Such solution leads straight to increasing of time-interval measurement. Knowing delay lines characteristics such as DNL (Differential Nonlinearity) and INL (Integral Nonlinearity) and using quantization-and-nonlinearity-minimization (QNM) method, it is possible to obtain two-sample-difference histogram, increase system resolution and decrease uncertainty of time-interval measurement [9].

2. ARCHITECTURE OF THE TIMS

TIMS as a virtual instrument consists of hardware unit flexible software and computer.

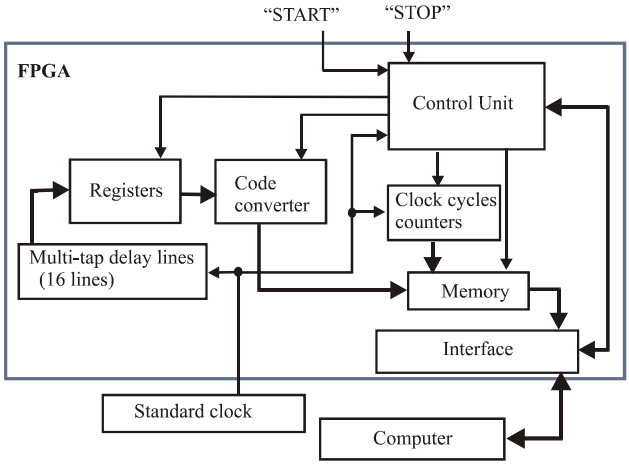

Fig.2. The block diagram of TIMS

The block diagram of the new TIMS architecture is shown in Fig.2. The system consists of the group of sixteen sixty-four-elements multi-tap delay lines with independent registers, code converter, two clock cycles counters, block of memory, interface and control unit. The TIMS can be implemented in a single Spartan or Virtex FPGA device. Implementation of TIMS in Virtex-4 device is shown in Fig.3.

In case, when the incoming pulses have different amplitudes two constant fraction discriminators should be applied according to the both Start and Stop inputs [10]. Application of the constant fraction discriminators decreases the pulse position error and increases the precision of the time-interval measurement.

Multiplication of the clock cycles counter ensures sufficient set-up time during incrementation and the data can be asynchronously read-out from one of the counter.

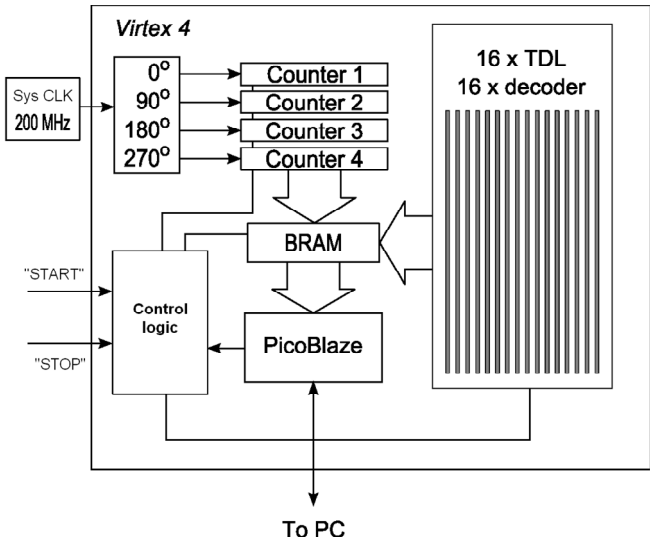

Fig. 3. TIMS implementation in Virtex-4 device

Code converter enables for data conversion to the natural binary code. In the presented measurement system single code converter is applied. Such solution significantly decreases FPGA resources used for implementation, however increases the total conversion time.

Each measured time stamp consists of main part, which is taken from one of the clock cycles counters and residual part, which is taken from one of the delay-line register through the data converter.

Curry chain of CLB's (Configurable Logical Block) is used to tapped delay lines and registers implementation, as it is shown in Fig. 4.

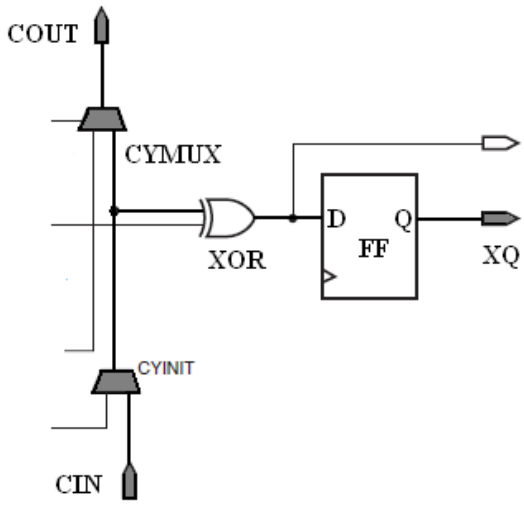

Fig. 4. Single delay-line element

Each delay line is placed in single FPGA column of CLB. Selection of appropriate delay elements is forced by the UCF (User Constrains File). Calibration of the delay-line elements is possible but not easy. First of all, the place of the delay-line can be changed by the choice of different CLB's column. Secondly, in each CLB, there are two slices which can be also replaced. Delay of individual element can

be increased by increasing the input capacity, which is possible by connection of additional elements in the system.

Architecture, which is described in this paper, is significantly different from the parallel architecture Bounce [12].

3. MULTI-TAPPED DELAY LINES UNIT

Even if the calibration process of the delay lines will run very precisely which is not always possible, the characteristics of the delay lines will be different. It means, that the time-bins in different lines have a different width.

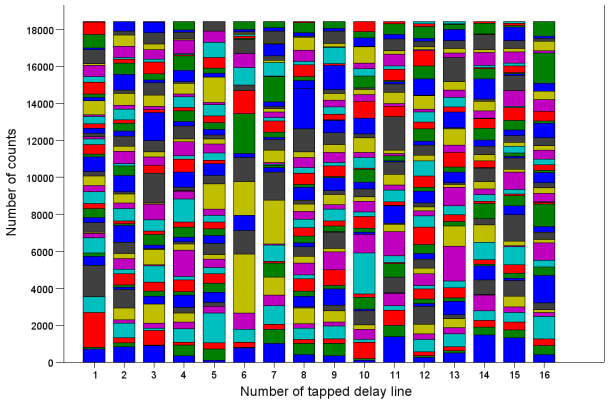

Fig.5. Comparison of the line delay characteristics

The widths of bins for sixteen delay-lines obtained using the statistical method [5, 6] are shown in Fig. 5.

However the characteristics of lines are not identical, the results of the time-intervals measurements has a Gaussian statistic, as it is shown in Fig. 6.

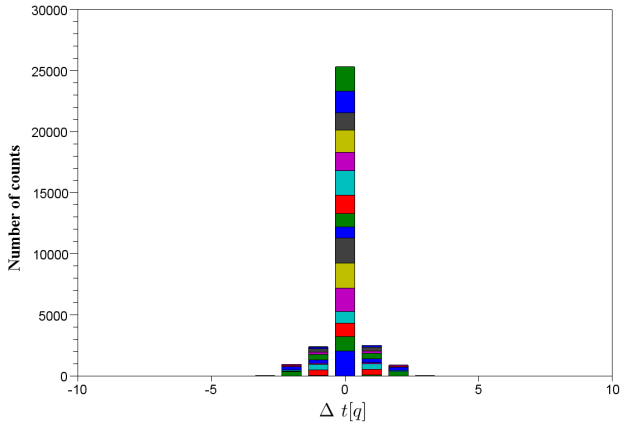

Fig.6. The time-intervals histogram

Assuming that residual time-intervals Δt_p, Δt_k are interpolated by sixteen independent delay lines it is possible to improve the system uncertainty four times. In practice, the interpolators are correlated and further improvement of the measurement uncertainty is possible [9].

4. TIME-INTERVAL HISTOGRAM CALCULATION

The simplest and the most effective way of time-interval (TI) histogram calculation when the multi-tapped-delay-line (MTDL) is being applied is the QNM method [9]. When the TIMS consists of n tapped-delay-lines (TDL) then for each time-interval, the time-interval histogram is updated n times. When all TDL characteristics are uncorrelated to each other, the time-interval histogram can be calculated even with n time greater precision.

For each time-interval, two time-stamps (TS) are being generated by each TDL. The contribution that is added to TI histogram equals to the modified convolution (the argument of the first function has been changed in sign [9]) of TS probability-density-functions (PDF).

Let the i-th TS be registered in $P_{k,i}$-th quantization step, the j-th TS be registered in $P_{k,j}$-th quantization step and $\sigma_{k,n}(t)$ be the PDF of n-th (all TDL considered) quantization step (Fig. 7). In this case, the value that should be added to time-interval histogram in range (t_1, t_2) for k-th TDL equals to

$$\rho_{k,i,j}(t_1,t_2) = \int_{t_1}^{t_2} \sigma_{E_{k,P_{k,i}}}(-\tau) \otimes \sigma_{E_{k,P_{k,j}}}(\tau) d\tau \,. \qquad (2)$$

When measurement module consists of n TDLs then for each TI, TI histogram in range $[t_1, t_2]$ is updated by sum of all contributions, so

$$\rho_{i,j}(t_1,t_2) = \sum_{k=0}^{n-1} \rho_{k,i,j}(t_1,t_2). \qquad (3)$$

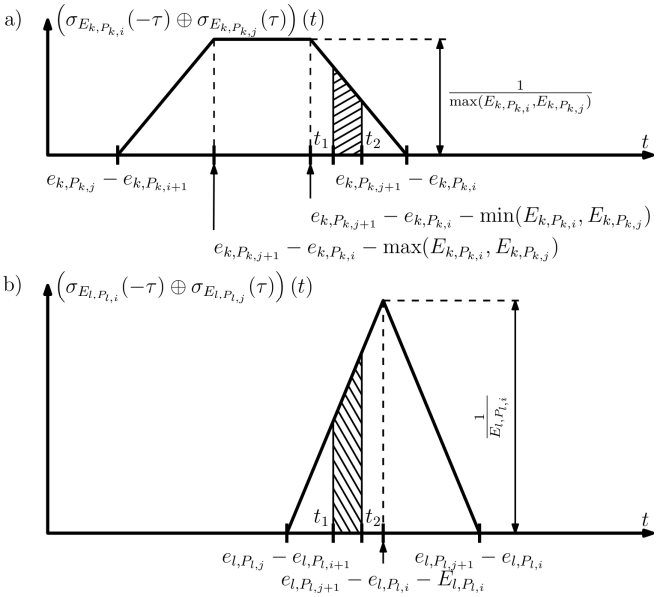

Fig.7. Two exemplary convolutions obtained as the result of time interval measurement between i-th and j-th pulses registered by k-th and l-th tapped delay lines; the quantization steps a) differ in width ($E_{k,P_{k,i}} \neq E_{k,P_{k,j}}$), b) are equal to each other ($E_{l,P_{l,i}} = E_{l,P_{l,j}}$)

Fig. 7, shows the calculation of contributions generated by k-th and l-th TDLs. The two quantization steps in k-th TDL into which the TS has been registered are different in width ($E_{k,P_{k,i}} \neq E_{k,P_{k,j}}$), so the PDF of this contribution is

trapezoidal (Fig. 7a). The contribution that is generated by l -th TDL is isometric triangular (Fig. 7b) because the widths of two TSs, into which the TI has been registered in this TDL, equal to each other ($E_{l,P_{l,i}} = E_{l,P_{l,j}}$).

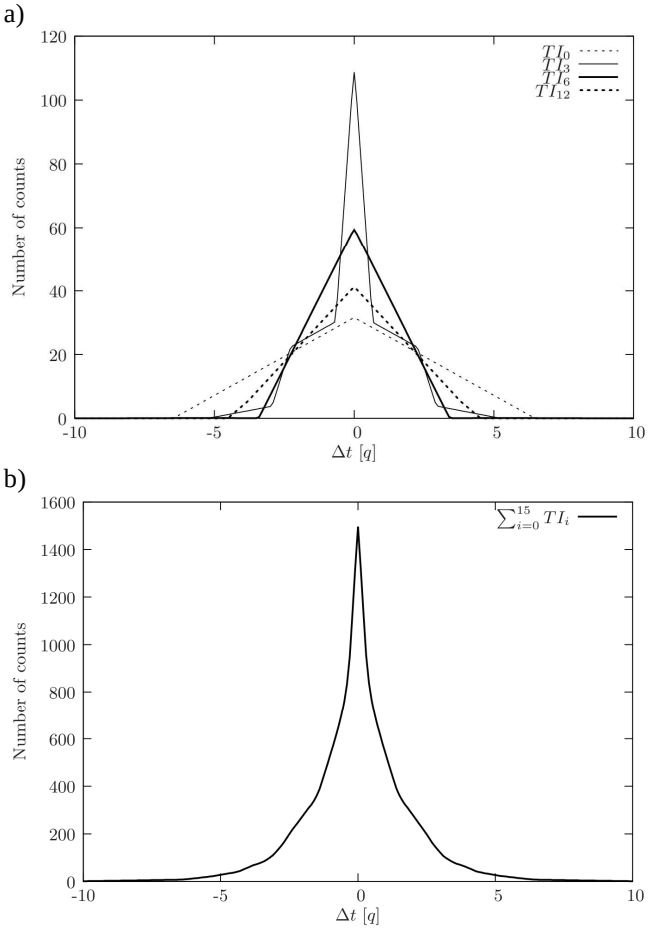

Fig.8. Time-interval histogram after QNM correction; a) contribution of histograms obtained separately from four randomly chosen TDLs, b) the resultant TI histogram

The contributions introduced by these two TDLs differ because of uncorrelated TDL characteristics. The area of rising pattern represents the contribution that is added by k -th TDL in range $[t_1, t_2]$ to the resultant TI histogram (Fig. 7a) and analogically the area of falling pattern is the contribution that is added by l -th TDL.

Application of the QNM method allows to obtain TI histogram where the position of the time peak is much more precise (Fig. 8b) than in TI histogram shown in Fig. 6.

Fig. 8a shows TI histograms obtained from four randomly chosen TDLs. The time unit was chosen to be equal to average value of quantization step, and the average value of peak position equals to zero because the information about the number of periods was removed.

4. TIME-INTERVAL MEASUREMENT

A series of time-interval measurements was performed to verify the new measurement system. For the test, a single section of coaxial cable was used as a delay element as it is shown in Fig.9.

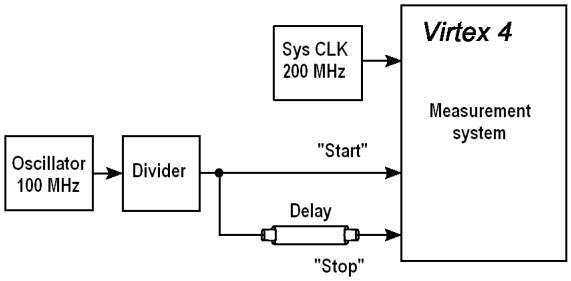

Fig.9. Verification of the measurement system

The results of time-interval measurements obtained during test are shown in Fig.10.

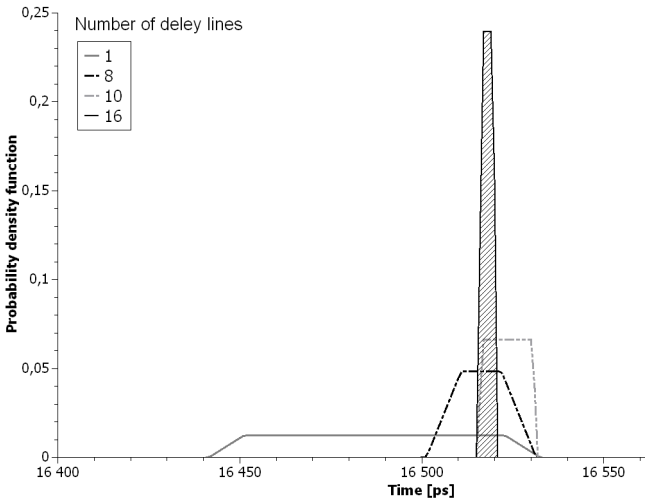

Fig.10. Probability density functions of measured time-intervals versus number of the TDL

Accuracy of time-interval determination increases when the number of TDL increases. Uncertainty of time-interval determination during single measuring cycle is about 50 ps when TIMS contains only single TDL but significantly decreases to several picoseconds when TIMS contains sixteen TDLs.

5. ERROR ANALYSIS

The time to digital converter, in system described above, consists of sixteen independent tapped delay lines. The delay of a single segment for each line can be calculated by the statistical method.

If we marked by N the total number of measurements made in a series, by $n_{i,j}$ number of data included in i-th channel and j-th line, then the delay of a single segment for the j-th line can be written as:

$$q_{i,j} = \frac{n_{i,j}}{N} T_0,\ i = \{0,1,...,M-1\},\ j = \{0,1,...,K-1\} \quad (4)$$

where T_0 is the system clock period and M is the number of time channels, and K is the number of tapped delay lines.

If all the time channels widths (within a single tapped delay line) are summed up, and divided by the number of the time channels, then it is possible to calculate the average time channels width.

$$\bar{q}_j = \frac{1}{M} \sum_{i=0}^{M-1} q_{i,j} \quad . \quad (5)$$

By subtracting the width of i-th channel from the average value, differential nonlinearity can be calculated as:

$$DNL_{i,j} = q_{i,j} - \bar{q}_j \quad . \quad (6)$$

Summing up the particular deviation from the average channel width, integral nonlinearity errors will be given (for each line) as:

$$INL_{i,j} = \sum_{i=0}^{M-1} DNL_{i,j} \quad (7)$$

The integral nonlinearity error determines how large an error during the measurement of time-interval, using this module, will be committed.

For a single delay line, a time-interval measure is described by equation [11]:

$$\Delta t_j = (n_j - m_j) \cdot \bar{q}_j + NT_0 \quad , \quad (8)$$

where m_j and n_j are the time channel numbers, for START and STOP pulses respectively, N is the total number of clock cycles, T_0 clock period.

Integral nonlinearity error is associated with each of time channels. Therefore the uncertainty, associated with time to digital converter characteristic, in a single time-interval measurement can be described as:

$$\sigma_{\Delta t_j} = \max\left\{\left|INL_{n,j}\right|, \left|INL_{m,j}\right|\right\} . \quad (9)$$

Moreover, the total uncertainty consists of an uncertainty connected with time-interval module characteristics, and a quantization error.

Assuming that, the constant time-interval Δt is measured, then two time intervals $T_1 = n_1\tau < \Delta t$ and $T_2 = n_1\tau + \tau > \Delta t$ are obtained, where τ is a time-interval measurement module resolution.

Introducing a new factor $c = n_1/N$, and defining it as a probability that the measured time-interval Δt will have a length T_1, and defining $q(T_2)$ as a probability that the measured time-interval Δt will have a length T_2, then following relationships are satisfied [1]:

$$p(T_1) = c \quad (10)$$

$$q(T_2) = 1 - c \quad (11)$$

The time-interval can be described as:

$$\Delta T = p(T_1) \cdot T_0 + q(T_2) \cdot T_0 \quad (12)$$

The standard deviation associated with quantization effect is given by:

$$\sigma_q = \tau \sqrt{p(T_1) \cdot q(T_2)} \quad (13)$$

In this way, the maximal error associated with quantization effect is defined as:

$$\sigma_q = \frac{\tau}{2} \quad . \quad (14)$$

LabView environment was used to prepare simulation, and obtained results are shown in Fig.11.

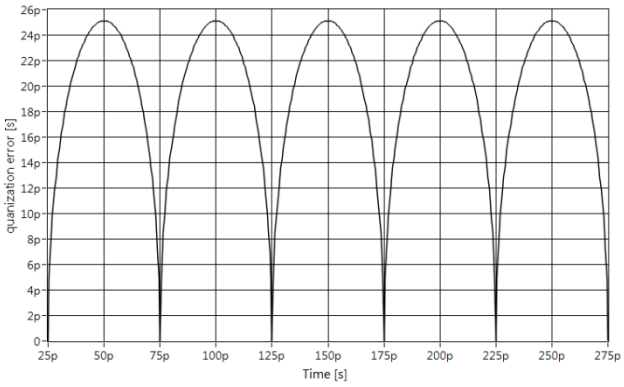

Fig.11. Quantization error as a function of channel width

The total uncertainty for j-th tapped delay line is described by relation:

$$\sigma_{all_j} = \sqrt{\sigma_{\Delta t_j}^2 + \sigma_{q_j}^2} \quad (15)$$

When the single time-interval Δt is measured by sixteen tapped delay lines, as a result of this measurement sixteen different time-intervals Δt_j are registered. Each of them has different uncertainty σ_{all_j}. Because each time- interval is measured with unequal precision, then the average time interval measured by sixteen tapped delay lines is described by equation:

$$\overline{\Delta t} = \frac{\sum_{j=0}^{K} \frac{\Delta t_j}{\sigma_{all_j}^2}}{\sum_{j=0}^{K} \frac{1}{\sigma_{all_j}^2}} \quad (16)$$

In fact, it is a weighted average value with weights:

$$w_j = \frac{1}{\sigma_{all_j}^2} \quad (17)$$

Two estimators of variance can be calculated. Internal variance:

$$\sigma_{\text{int}}^2 = \frac{1}{\sum_{j=0}^{K} \frac{1}{\sigma_{all_j}^2}} \quad (18)$$

and the external variance:

$$\sigma_{ext}^2 = \frac{\sigma_{\text{int}}^2}{K} \sum_{j=0}^{K} \left(\frac{\Delta t_j - \overline{\Delta t}}{\sigma_{all_j}} \right)^2 \quad (19)$$

Internal and external variance, during the experimental process, can be different. When this occurs, then the larger of them is chosen:

$$\sigma^2_{\overline{\Delta t}} = \max\left\{\sigma^2_{\text{int}}, \sigma^2_{ext}\right\} \quad (20)$$

The uncertainty of a single time-interval measurement was verified using a virtual time interval measurement system with real module characteristics. Results of this investigations are shown in Tab. 1.

Tab.1. A single time-interval measurement uncertainty using a single σ_{all_j} and sixteen delay lines $\sigma_{\overline{\Delta t}}$.

j	$\sigma_{all_j}[ps]$	j	$\sigma_{all_j}[ps]$	$\sigma_{\overline{\Delta t}}[ps]$
0	174.1	8	109.0	30.9
1	149.1	9	152.1	
2	137.2	10	129.6	
3	143.2	11	100.5	
4	107.9	12	117.5	
5	109.8	13	101.9	
6	130.7	14	104.0	
7	128.1	15	175.8	

6. SUMMARY AND CONCLUSIONS

Implementation of the time-interval measuring module in the FPGA devices allows to greatly increase the scale of system integration. Moreover, using the multi-tap delay lines technique enables to significantly increase the system resolution. Application of the QNM method and implementation of the tapped delay lines using the carry path, allow to obtain the system resolution of picoseconds. Such resolution can significantly improve the quality of time-of-flight mass spectrometers, ultrasonic flowmeters and life-time measuring systems.

The authors also want to point out that application of the programmable logical devices, especially the FPGA devices, increases the flexibility and reliability of the measuring system.

Acknowledgments

This work was supported by the Polish National Science Centre (NCN) Grant No N N505 484540

5. REFERENCES

[1] J. Kalisz, "Review of methods for time interval measurements with picosecond resolution", Metrologia, no. 41, pp 17-32, 2004.

[2] W. Zhou, X. Ou, H. Zhou, B. Wang, X. Yang, "A Time Interval Measurement Technique Based on Time – Space Relationship Processing", IEEE Int. Freq. Contr. Symp. and Exposition, pp. 260-266, June 2006.

[3] J. Song, Q. An, and S. Liu, "A High-Resolution Time-to-Digital Converter Implemented in Field-Programmable-Gate-Arrays", IEEE Trans. On Nucl. Sci., vol. 53, no. 1, pp. 236-241, Feb. 2006.

[4] M. Zieliński, "Review of single-stage time-interval measurement modules implemented in FPGA devices", Metrology and Measurement Systems, vol XVI, no.4, pp 641-647, 2010.

[5] M. Zieliński, D. Chaberski, S. Grzelak, „Time-interval measuring modules with short deadtime", Metrology and Measurement Systems, vol. X no. 3, pp. 241 – 251, 2003.

[6] M. Zieliński, D. Chaberski, M. Kowalski, R. Frankowski and S. Grzelak, „High-resolution time-interval measuring system implemented in single FPGA device", Measurement, vol 35, no. 3, pp. 311 – 317, 2004.

[7] M. Zieliński, M. Kowalski, R. Frankowski, D. Chaberski, S. Grzelak and L. Wydźgowski, "Accumulated jitter measurement of standard clock oscillators", Metrology and Measurement Systems, vol. XVI, no. 2, pp. 259 – 266, 2009.

[8] W. Wasilewski, P. Kolenderski, R. Frankowski, "Spectral density matrix of a single photon measured", Phys. Rev. Lett. vol. 99, no. 12, p. 123601, 2007.

[9] M. Zieliński, D. Chaberski, S. Grzelak, „The new method of calculation sum and difference histogram for quantized data", Measurement vol. 42, no. 9, pp. 1388 – 1394, 2009.

[10] M. Zieliński, D. Chaberski, S. Grzelak, R. Frankowski and M. Kowalski, "High-resolution real-time multichannel scaler implemented in single FPGA device", XVII IMEKO World Congress, Dubrovnik, Croatia, pp. 708 – 711, 2003.

[11] R. Pełka, J. Kalisz, R. Szplet, Nonlinearity correction of the integrated time-to-digital converter with direct coding. IEEE Trans. Instrum. Meas., 46(2):449–452, April 1997.

[12] R. Joost, R. Salomon: "BOUNCE, a Concept to Measure Picosecond Time Intervals with Standard Hardware". Emerging Technologies and Factory Automation, ETFA 2008. IEEE International Conference, Sept. pp. 1010-1015, 2008.